Ultrahigh-Q Tunable Whispering-Gallery-Mode Microresonator

M. Pöllinger, D. O'Shea, F. Warken, and A. Rauschenbeutel*

Institut für Physik, Johannes Gutenberg-Universität Mainz, 55099 Mainz, Germany

(Received 30 January 2009; revised manuscript received 23 April 2009; published 28 July 2009)

Typical microresonators exhibit a large frequency spacing between resonances and a limited tunability. This impedes their use in a large class of applications which require a resonance of the microresonator to coincide with a predetermined frequency. Here, we experimentally overcome this limitation with highly prolate-shaped whispering-gallery-mode "bottle microresonators" fabricated from standard optical glass fibers. Our resonators combine an ultrahigh quality factor of 3.6×10^8, a small mode volume, and near-lossless fiber coupling, characteristic of whispering-gallery-mode resonators, with a simple and customizable mode structure enabling full tunability.

DOI: 10.1103/PhysRevLett.103.053901 PACS numbers: 42.60.Da, 42.50.Pq, 42.79.−e

Optical microresonators hold great potential for many fields of research and technology [1]. They are used for filters and switches in optical communications [2–4], nonlinear optics [5], bio(chemical) sensing [6], microlasers [7–9], as well as for cavity quantum electrodynamics applications such as single photon sources [10–12] and interfaces for quantum communication [13,14]. All these applications rely on the spatial and temporal confinement of light by the microresonator, characterized by its mode volume V and its quality factor Q, respectively [1]. The ratio Q/V thus defines a key figure relating the coupling strength between light and matter in the resonator to the dissipation rates of the coupled system. The highest values of Q/V to date have been reached with whispering-gallery-mode (WGM) microresonators [15]. Standard WGM microresonators, like dielectric microspheres, microdisks, and microtori, typically confine the light in a narrow ring along the equator of the structure by continuous total internal reflection at the resonator surface [16]. While such equatorial WGMs have the advantage of a small mode volume they also exhibit a large frequency spacing between consecutive modes. In conjunction with the limited tuning range due to their monolithic design, tuning of equatorial WGM microresonators to an arbitrary frequency has therefore not been realized to date.

For this reason, the WGM "bottle microresonator" has recently received considerable attention [17–20] because it promises a customizable mode structure while maintaining a favorable Q/V ratio [21,22]. Because of its highly prolate shape, the bottle microresonator gives rise to a class of whispering-gallery-modes (WGMs) with advantageous properties, see Fig. 1(a). The light in these "bottle modes" harmonically oscillates back and forth along the resonator axis between two turning points which are defined by an angular momentum barrier [22]. The resulting axial standing wave structure exhibits a significantly enhanced intensity at the so-called "caustics" of the bottle mode, located at the turning points of the harmonic motion. The bottle microresonator possesses an equidistant spectrum of eigenmodes, labeled by the "azimuthal quantum number" m, which counts the number of wavelengths that fit into the circumference of the resonator, and the "axial quantum number" q, which counts the number of axial intensity nodes [21,22]. The frequency spacing between modes with

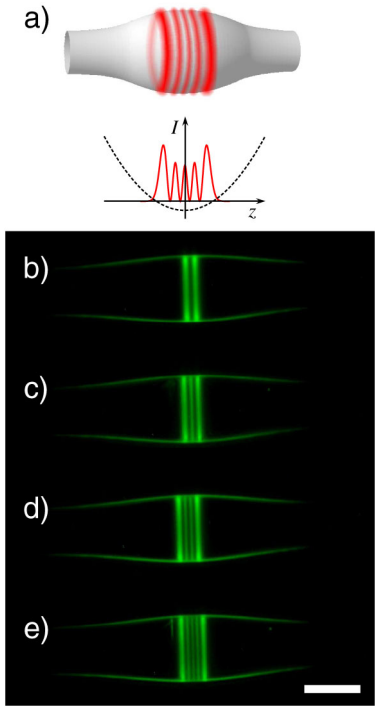

FIG. 1 (color online). (a) Concept of the bottle microresonator. In addition to the radial confinement by continuous total internal reflection at the resonator surface, the axial confinement of the light is caused by an effective harmonic potential (dashed line) fixed by the curvature of the resonator profile. The resulting intensity distribution is therefore given by the eigenfunctions of the quantum mechanical harmonic oscillator [22]. (b)–(e) Experimental micrographs of the $q = 1 - 4$ bottle modes visualized via the up-converted green fluorescence of dopant erbium ions in a 36-μm diameter bottle microresonator. Scale bar, 30 μm.

consecutive quantum numbers q (m) is called the axial (azimuthal) free spectral range and will be denoted $\Delta\nu_q$ ($\Delta\nu_m$) in the following.

In small WGM resonators the azimuthal free spectral range (FSR) is typically very large. For example, changing m by one for a 35-μm diameter WGM changes its resonance frequency by $\Delta\nu_m \approx 2$ THz, i.e., about 1% of the optical frequency. Tuning a WGM microresonator over such a large range is a critical issue. Exploiting the temperature dependence of the refractive index of silica, electrical thermo-optic tuning of equatorial WGMs in a 75-μm diameter microtorus over more than 300 GHz, i.e., up to 35% of the azimuthal FSR, has been demonstrated [23]. Another tuning scheme involves elastically deforming the resonator through mechanical strain, thereby changing its diameter and the refractive index of the medium. Using this strain tuning technique, tuning over 400 GHz (50% of the azimuthal FSR) has been demonstrated for a 80-μm diameter microsphere, limited by the mechanical damage threshold of the resonator [24]. The bottle microresonator circumvents this problem: Its axial FSR only depends on the curvature of the resonator profile and can thus be made significantly smaller than its azimuthal FSR [22]. It is therefore sufficient to tune the bottle microresonator over one axial FSR in order to ensure that an arbitrary predetermined frequency will coincide with the resonance frequency of an appropriately chosen bottle mode.

Previous experimental work has demonstrated that bottle microresonators are readily fabricated from standard optical glass fibers with an initial diameter of 125 μm in a two-step heat-and-pull process [17–19]: First, a few millimeters long section with a homogeneous diameter is created by elongating the fiber while heating the section with a traveling flame or a scanned CO_2-laser beam. Next, a bulge is created on the tapered fiber waist which is located between two microtapers. Each of the microtapers is realized by locally heating the tapered fiber waist with a focussed CO_2-laser beam while slightly stretching it. The resulting bulge forms the bottle microresonator which exhibits a parabolic variation of the fiber diameter $D(z) \approx D_0[1 - (\Delta k z)^2/2]$ around its central zone, where D_0 is the maximum diameter of the bulge at the position $z = 0$ along the resonator axis and Δk denotes the curvature of the resonator profile. So far, the values for D_0 ranged from 12 μm [18] to 16 μm [17,19]. Theoretically, these values should be large enough to avoid radiative losses and thus to reach Q factors in the 10^7–10^9 range [25]. However, the experimentally observed Q factors were smaller than 10^4 in [17]. In our own work, we observed a strong decrease of the Q factor for diameters below $D_0 \approx 30$ μm, in agreement with the results obtained on microtori [15]. Therefore, the bottle microresonators used here have a diameter of $D_0 = 30$–40 μm. We reconstruct the diameter profile with a precision of ± 2 μm using a microscope in combination with a customized image analysis software. This method allows us to determine Δk with a precision of ± 0.001 μm^{-1}. Adjustment of the CO_2-laser beam spot-size, the microtaper separation, and the elongation length allows us to precisely tailor the resonator shape and thereby customize its mode structure. Typically, we work with a curvature of $\Delta k = 0.010$–0.015 μm^{-1}.

The spatial and spectral properties of the modes are investigated using a distributed feedback (DFB) diode laser operating around 850 nm with a short-term (<5 μs) linewidth of 400 kHz. Efficient coupling of propagating light fields to the bottle modes requires phase matched excitation. We couple light in and out by means of a submicron sized tapered ''coupling fiber'' [26]. It is fabricated by a similar heat-and-pull technique as described above and is aligned perpendicularly to the resonator axis at one of the caustics of a particular axial mode. Its radius is chosen for optimized phase matching to the lowest order radial modes which exhibit the smallest mode volume and the highest evanescent field at the surface of the resonator [26]. The gap between the coupling fiber and the resonator is comparable to the decay lengths of the evanescent fields of both structures, i.e., a few hundred nanometers, and is controlled with a resolution of 10 nm using a piezoelectric actuator. For coupling to different axial modes the position of the coupling fiber can be scanned along the resonator axis via a servomotor-driven translator with 100 nm resolution. By carefully adjusting the coupling fiber-resonator gap, we realize so-called critical coupling where the incident optical power is entirely dissipated in the resonator and the transmission of the coupling fiber at resonance ideally drops to zero [27]. In addition, we experimentally observe near-unity values ($>99.5\%$) for the ideality [28] of our fiber taper coupler. This means that the coupling junction between the fiber taper and the bottle microresonator introduces only very weak losses. Unity ideality holds huge importance for a wide range of applications where near-lossless transfer of light to and from the resonator mode is a requisite.

In order to characterize the spatial properties of the bottle modes we fabricate an erbium doped resonator with $D_0 = 36$ μm and $\Delta k = 0.015$ μm^{-1} from the 50-μm diameter core of a standard Er^{3+}-doped multimode fiber, whose cladding is removed by wet etching. When resonantly exciting bottle modes around 850 nm, the erbium ions emit fluorescence light around 540 nm in an up-conversion process [8,9]. This green fluorescence is then observed using an optical microscope. Depending on the position of the coupling fiber along the resonator axis and the laser frequency different axial modes can be individually excited, see Figs. 1(b)–1(e). Each picture has been generated from a stack of micrographs obtained by varying the focal plane in order to increase the effective focal depth. The measured intensity distribution confirms the axial standing wave structure and the enhanced light intensity at the caustics which are at the heart of the bottle microresonator concept [20,22].

Next, we determine the quality factor $Q = \omega\tau$ of an undoped resonator, where τ is the photon lifetime in the

resonator and $\omega = 2\pi\nu$ is the optical frequency. For this purpose, we use a cavity ringdown technique: We resonantly excite the bottle mode under investigation with the 850 nm probe laser at critical coupling. After switching off the probe beam within 35 ns using an acousto-optical modulator, the exponential decay of the intracavity power is monitored through the output port of the coupling fiber. This measurement, shown in Fig. 2(a), is taken on a resonator with $D_0 = 35\ \mu$m and $\Delta k = 0.012\ \mu\text{m}^{-1}$ and yields a photon lifetime at critical coupling of $\tau_{\text{crit}} = 82$ ns. We thus obtain a lower bound for the intrinsic photon lifetime in the uncoupled resonator of $\tau_0 = 2\tau_{\text{crit}} = 164$ ns [15] and an intrinsic quality factor in excess of $Q_0 = 3.6 \times 10^8$. This ultrahigh intrinsic quality factor is comparable to the values reported for other WGM microresonators of the same diameter [15]. Spectral measurements, which are, however, affected by thermal bistability, confirm this result; see Fig. 2(b). We note that at critical coupling, required for many applications, our quality factor of $Q_{\text{crit}} = \omega\tau_{\text{crit}} = 1.8 \times 10^8$ is about 1 order of magnitude larger than what has previously been reported [15]. Several measurements on different resonators showed similar quality factors, independent of the axial quantum number. Figure 2(c) shows a wide range transmission spectrum of a bottle microresonator. The coupling to the $q = 0$ and $q = 1$ bottle modes was selectively maximized by optimizing the phase-matching, resulting in an advantageously low spectral mode density. The q quantum numbers of the modes were identified in a separate measurement by translating the coupling fiber along the resonator axis while recording the spatial modulation of the coupling efficiency.

We now demonstrate strain tuning of a bottle microresonator using the setup depicted in Fig. 3(a). The measurement was carried out with the 35-μm diameter bottle microresonator which yielded the ultrahigh Q factor in the above ringdown measurement. In Fig. 3(b) the resonance frequencies of the $q = 1$ and $q = 2$ bottle modes were measured for varying mechanical strain. The so determined tuning range of 700 GHz corresponds to 700 000 linewidths of the resonator and is 1.7 times larger than the axial FSR. The experimentally measured axial FSR of $\Delta\nu_q = 425 \pm 8$ GHz is in good agreement with the theoretical value of 397 ± 33 GHz, calculated from the measured curvature of the resonator profile. The maximum stress applied to the resonator in this measurement, limited by the travel range of the bending actuator, can be inferred from the frequency shift and was about 35% of the typical damage threshold of the silica resonator structure [29]. The bottle microresonator can thus be tuned to an arbitrary frequency by strain tuning the nearest axial bottle mode. However, in order to keep the mode volume small it is desirable to work with a low axial quantum number q, thereby minimizing the separation between the two caustics; see Figs. 1(b)–1(e). Remarkably, this is possible for the bottle microresonator which exhibits two FSRs, axial and azimuthal, and which can thus be tuned to any arbitrary frequency using, e.g., only the $q = 1 - 4$ axial bottle modes which allow us to bridge the azimuthal FSR. These four lowest order bottle modes have a calculated mode volume ranging from 1180 μm^3 to 1470 μm^3 for a wavelength of $\lambda \approx 850$ nm, corresponding to $6070(\lambda/n)^3$ to $7560(\lambda/n)^3$, where $n = 1.467$ is the index of refraction of silica. This results in an intrinsic Q/V value of up to $5.9 \times 10^4(\lambda/n)^{-3}$ which remains as high as $3.0 \times 10^4(\lambda/n)^{-3}$ in the case of critical coupling. These numbers are high enough to realize light-matter interaction deep

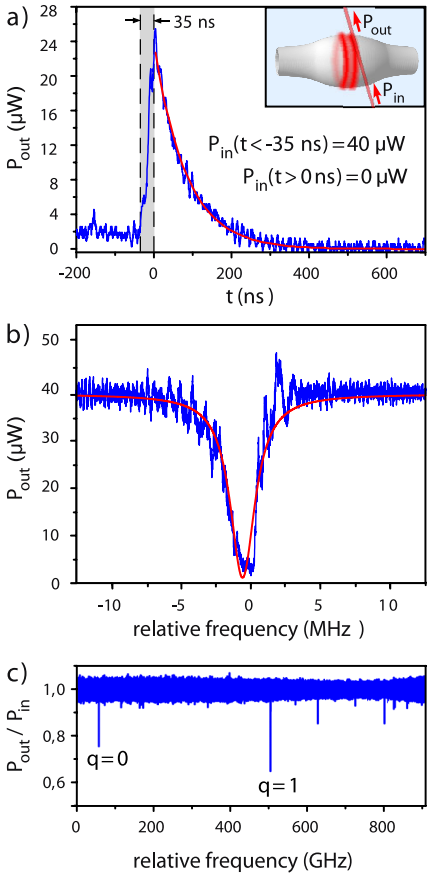

FIG. 2 (color online). (a) Cavity ringdown measurement of the $q = 1$ bottle mode in a bottle microresonator with 35 μm diameter and a curvature of $\Delta k = 0.012\ \mu\text{m}^{-1}$ at critical coupling for a wavelength near 850 nm and transverse electric (TE) polarization, i.e., with the magnetic field parallel to the resonator surface. The inset schematically shows the coupling geometry with the submicron coupling fiber aligned with one of the two caustics of the bottle mode. (b) Spectrum of a 38 μm-diameter bottle microresonator with $\Delta k = 0.009\ \mu\text{m}^{-1}$, obtained by scanning the probe laser frequency over the resonance of a $q \approx 30$ bottle mode at critical coupling. The solid line is a Lorentzian fit yielding a FWHM linewidth of 2.1 ± 0.1 MHz, corresponding to an intrinsic quality factor in excess of $Q_0 = 3.3 \times 10^8$. Because of the presence of optical bistability the measured line is slightly asymmetric and broadened. (c) Wide range transmission spectrum showing both the $q = 0$ and $q = 1$ bottle mode in a 37 μm-diameter bottle microresonator with $\Delta k = 0.012\ \mu\text{m}^{-1}$.

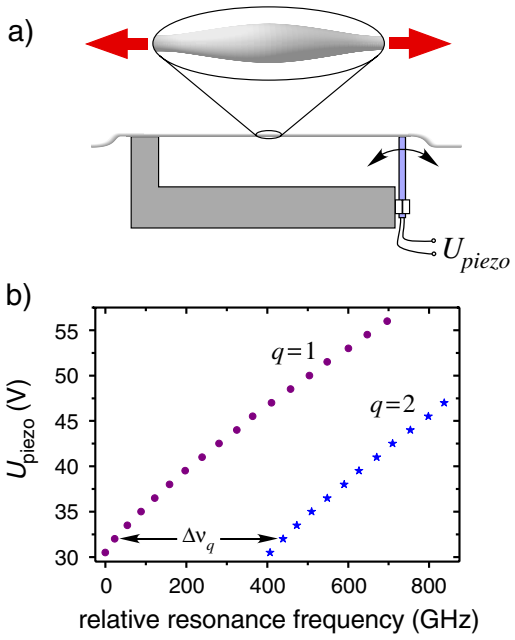

FIG. 3 (color online). (a) Design of the mount for applying mechanical strain to the bottle microresonator. The fiber that contains the resonator structure is attached to a piezoelectric bending actuator which elastically elongates the fiber and is controlled by a voltage U_{piezo}. (b) Strain tuning of the TE polarized $q = 1$ and $q = 2$ bottle modes of the same bottle microresonator as used in Fig. 2(a). The tuning range of 700 GHz of the $q = 1$ mode exceeds the observed axial FSR of $\Delta\nu_q = 425 \pm 8$ GHz by a factor of 1.7.

within the so-called strong coupling regime. For example, the atom-field coupling rate between a cesium atom and the $q = 1$ bottle mode near the surface of the resonator is calculated to be $g = 2\pi \times 50$ MHz which clearly exceeds the dissipation rates of the system, given by the cavity field decay rate $\kappa = \omega/2Q_0 = 2\pi \times 0.49$ MHz and the transverse atomic dipole decay rate $\gamma_\perp = 2\pi \times 2.6$ MHz.

Summarizing, we present a fully tunable whispering-gallery-mode microresonator. The tunability of our bottle microresonator stems from the confinement of the light between two caustics in a simple axial mode structure. In conjunction with its high Q/V value this reveals the enormous potential of the bottle microresonator for coupling light and matter. Moreover, the advantageous mode geometry of the bottle modes allows near-lossless simultaneous coupling of two independent coupling fibers at the two caustics and thus to induce a resonator-mediated nonlinear interaction between two distinct optical signals at the single photon level. The bottle microresonator thereby opens the route towards the realization of next-generation communication and information processing devices such as single photon all-optical switches [30] and single photon transistors [31].

The authors wish to thank W. Alt and D. Meschede for their valuable support and in-depth discussions. Financial support by the DFG (Research Unit 557), the Volkswagen Foundation, and the ESF (EURYI) is gratefully acknowledged.

*rauschenbeutel@uni-mainz.de

[1] K. J. Vahala, Nature (London) **424**, 839 (2003).
[2] K. Djordjev, S. J. Choi, and P. D. Dapkus, IEEE Photonics Technol. Lett. **14**, 828 (2002).
[3] S. T. Chu *et al.*, IEEE Photonics Technol. Lett. **11**, 691 (1999).
[4] V. R. Almeida, C. A. Barrios, R. R. Panepucci, and M. Lipson, Nature (London) **431**, 1081 (2004).
[5] P. Del'Haye *et al.*, Nature (London) **450**, 1214 (2007).
[6] A. M. Armani, R. P. Kulkarni, S. E. Fraser, R. C. Flagan, and K. J. Vahala, Science **317**, 783 (2007).
[7] V. Sandoghdar *et al.*, Phys. Rev. A **54**, R1777 (1996).
[8] W. von Klitzing *et al.*, J. Opt. B **2**, 204 (2000).
[9] M. Cai, O. Painter, and K. J. Vahala, Opt. Lett. **25**, 1430 (2000).
[10] P. Michler *et al.*, Science **290**, 2282 (2000).
[11] J. McKeever *et al.*, Science **303**, 1992 (2004).
[12] M. Hijlkema *et al.*, Nature Phys. **3**, 253 (2007).
[13] A. D. Boozer, A. Boca, R. Miller, T. E. Northup, and H. J. Kimble, Phys. Rev. Lett. **98**, 193601 (2007).
[14] T. Wilk, S. C. Webster, A. Kuhn, and G. Rempe, Science **317**, 488 (2007).
[15] T. J. Kippenberg, S. M. Spillane, and K. J. Vahala, Appl. Phys. Lett. **85**, 6113 (2004).
[16] A. B. Matsko and V. S. Ilchenko, IEEE J. Sel. Top. Quantum Electron. **12**, 3 (2006).
[17] G. Kakarantzas, T. E. Dimmick, T. A. Birks, R. Le Roux, and P. St. J. Russell, Opt. Lett. **26**, 1137 (2001).
[18] J. M. Ward, D. G. O'Shea, B. J. Shortt, M. J. Morrissey, K. Deasy, and S. G. Nic Chormaic, Rev. Sci. Instrum. **77**, 083105 (2006).
[19] F. Warken, A. Rauschenbeutel, and T. Bartholomäus, Photonics Spectra **42**, No. 3, 73 (2008).
[20] Ch. Strelow *et al.*, Phys. Rev. Lett. **101**, 127403 (2008).
[21] M. Sumetsky, Opt. Lett. **29**, 8 (2004).
[22] Y. Louyer, D. Meschede, and A. Rauschenbeutel, Phys. Rev. A **72**, 031801(R) (2005).
[23] D. Armani, B. Min, A. Martin, and K. J. Vahala, Appl. Phys. Lett. **85**, 5439 (2004).
[24] W. von Klitzing, R. Long, V. S. Ilchenko, J. Hare, and V. Lefèvre-Seguin, Opt. Lett. **26**, 166 (2001).
[25] J. R. Buck and H. J. Kimble, Phys. Rev. A **67**, 033806 (2003).
[26] J. C. Knight, G. Cheung, F. Jacques, and T. A. Birks, Opt. Lett. **22**, 1129 (1997).
[27] M. Cai, O. Painter, and K. J. Vahala, Phys. Rev. Lett. **85**, 74 (2000).
[28] S. M. Spillane, T. J. Kippenberg, O. J. Painter, and K. J. Vahala, Phys. Rev. Lett. **91**, 043902 (2003).
[29] G. S. Glaesmann and D. J. Walther, Opt. Eng. (Bellingham, Wash.) **30**, 746 (1991).
[30] P. Bermel, A. Rodriguez, S. G. Johnson, J. D. Joannopoulos, and M. Soljačić, Phys. Rev. A **74**, 043818 (2006).
[31] D. E. Chang, A. S. Sorensen, E. A. Demler, and M. D. Lukin, Nature Phys. **3**, 807 (2007).